

Equatorial Indian Ocean productivity during the last 33 kiloyears and possible linkage to Westerly Jet variability

Vikesano R. Punyu, Virupaxa K. Banakar*, Anita Garg

CSIR-National Institute of Oceanography, Dona Paula-403004, Goa, India

Abstract

The top 1 m radiocarbon dated section of a 5.6 m long sediment core retrieved from the Equatorial Indian Ocean is studied for productivity changes in response to climate variability that have taken place during the last ~33 kyr. The robust indicators of marine productivity such as phytol and brassicasterol exhibit distinctly higher contents (av. 5.8 ng/g and 4.8 ng/g respectively) during the LGM (25-17 ky BP) as compared to the succeeding period (16-5 ky BP: av. 1.9 ng/g each) and preceding period (33-25 ky BP: av. 1.8 and 0.8 ng/g respectively) suggest increased productivity during the cold and dry climate of the LGM. The C_{org} content is also relatively higher during this period than the warmer Holocene. However, marginally higher C/N ratios (~7.8) and enrichment of $\delta^{13}C_{org}$ (~ -19.8 ‰) during the LGM than the Holocene (C/N ~6.4 and $\delta^{13}C_{org}$ ~ -21.5 ‰), and also the higher carbon preference index (CPI) of *n*-alkanes and *n*-alkanols together suggest the presence of terrestrial organic matter in the sediment. The increased equatorial productivity and terrestrial organic matter input together during the LGM may indicate intensified inter-monsoon equatorial westerly jets resulting in elevated productivity.

*Corresponding author : email: banakar@nio.org

Key-words : Equatorial Indian Ocean; Palaeoproductivity ; Biomarkers ; Last Glacial Maximum ; Westerly Jets

1. Introduction

The Equatorial Indian Ocean (EIO) experiences altogether different wind-stress and productivity pattern compared to the rest of the northern Indian Ocean. The zonal winds in the EIO are mostly westerly throughout the year and reach their maximum during the spring and fall (inter-monsoon periods) generating a burst of intense eastward equatorial currents (Westerly Jets or Wyrтки Jets: “WJ”: Wyrтки, 1973; Senan et al., 2003). The WJ are active in a narrow band between 2°N to 2°S latitudes and 65° and 85°E longitudes. The dynamics of these easterly WJ force thermocline to shoal-up at its periphery on either side of the equator and in western-EIO, while deepening along the Equator and in eastern-EIO (see Figure 1). The WJ not only result in enhancement of the equatorial productivity (Beaufort et al., 1997; Cayre et al., 1999) (see Figure 2), but also appear to dictate the Equatorial Indian Ocean Oscillations that is believed to determine the strength of summer monsoon rainfall (Gadgil et al., 2003). These ocean-atmosphere coupled processes are believed to have connection with much larger regional climate systems such as Indian Ocean Dipole (IOD), El Nino-Southern Oscillations and North Atlantic Oscillations (Krishna Kumar et al., 1999; Chang et al., 2001; Roy, 2011).

Several previous studies based on time-series of sedimentary proxies from northern Indian Ocean have indicated that the past variations in the Indian monsoons were driven by high-latitude climates (see Schulz et al., 1998; Banakar et al., 2010; Hong et al., 2003 and references therein). One of the salient features of the monsoon forcing is the strong upwelling and associated enhanced productivity in the Arabian Sea (Haake et al., 1993). Lipid biomarkers are less susceptible than bulk organic matter to post-depositional alteration and offer many potential molecules for reconstructing the past productivity (Brassell, 1993; Volkman, 2006).

An unchanged phytoplankton community structure in the Arabian Sea for the past 200 kyr was suggested based on lipid biomarkers (Schubert et al., 1998). Schulte and Baard, (2003) and Schulte et al. (1999) have demonstrated increased productivity during the glacial periods of the last ~300 kyr utilising lipids extracted from sediment cores of North-West Indian Ocean. An association of productivity based on lipid biomarker with the solar irradiance has been observed for the last ~700 y in the Eastern Arabian Sea (Kurian et al. 2009). The brassicasterol concentration from sediment cores from different depths and locations from the North-West Indian Ocean has shown increased opal (diatom) production during glacial periods (Schulte et al., 1999). These previous studies demonstrate the potential of sedimentary lipid biomarkers as proxies for paleoproductivity.

In this study, we reconstruct the time-series of a suite of lipid biomarkers along with bulk organic matter and stable isotopes for the last ~33 kiloyears in a sediment core retrieved from the EIO, which falls within the realm of WJ. Therefore, it is feasible to retrieve the record of past variation in the intensity of these easterly jets through productivity reconstruction utilizing sedimentary biomarkers as the WJs can induce significant changes in the thermocline across and along the equatorial region.

2. Materials and methods

The 5.62 m long gravity core CC2-GCEq2 was retrieved at 2°29' N latitude and 78°E longitude on board R. V. A. A. Sidorenko Cruise-65 from a water depth of 3788 m (Figure 1). The sediment core location falls within the influence of modern intense WJ (Figure 1), and hence well suited to understand the past variation of the jet. The upper 100 cm which has been dated by the radiocarbon in October 2008 at NSF-AMS Facility of Arizona University, USA, was used for the present study. The radiocarbon dates were corrected for reservoir age of 600 y (<http://intcal.qub.ac.uk>) and converted to calendar age using CalPal2007-HULU on-line Calibration (Danzeglocke et al., 2008) (see Table 1). The radiocarbon dated sediment section corresponds to a maximum age of ~33 ky BP (Figure 3). The sediment core was sub-sectioned at 2 cm intervals on board and preserved under -20°C until transported to the land-based laboratory and freeze-dried. Alternative sections were utilized in the present study. The core top section recorded an age of 5204 ± 105 y BP suggesting that the Late Holocene record is missing. However, this loss does not prevent us to understand the relative variation in the equatorial production at two extreme climate conditions (LGM and Holocene).

Around twenty clean and intact tests of 250-350 μ size *Globigerinoides ruber* were picked under microscope and subjected to initial cleaning for oxygen isotope measurements an in-house Micromass IR-MS facility and the results are expressed relative to PDB in ‰ unit. The precision of six replicate measurements is 0.08 ‰. For C_{org}, N_{Tot} and δ¹³C_{org} measurements, the decarbonised samples were analyzed in in-house Thermo Flash-1112 elemental analyzer coupled with Delta-V Plus IR MS facility. The δ¹³C is expressed relative to PDB in ‰. The analytical accuracy of reference standard was within ± 2 ‰ for C_{org} and N_{Tot} and the measurement precision for δ¹³C_{org} is 0.2 ‰.

The total lipids (TL) were extracted following the method of Bligh and Dyer (1959) and estimated following Harji et al. (2008), and expressed as ng/g of dry sediment. In brief, a 15 gm of

homogenized sediment sample was used for separation of organic phase. The TL extracts further subjected to column chromatography to extract various lipids. The *n*-alkane fraction was adjusted to a final volume after adding methyl nonadecanoate as the internal standard. The *n*-alkanol + sterol fraction was evaporated and the residue was treated with 400 μ l mixture of the bistrimethyl-silyl-trifluoroacetamide (BSTFA) and pyridine (Supelco; 1:3, v/v) and silylated at 50 °C for 1 h in the oven. All the fractions were analyzed on a Shimadzu QP-2010 GC-MS equipped with RTX-5MS. The identification of the compounds was done by comparing the retention time of the compounds with the authentic standards of *n*-alkanes (C₁₃-C₃₃), *n*-alcohols (C₁₄-C₃₂ + phytol) and sterols (brassicasterol) of Supelco, USA. The quantification of individual compounds was done by peak area integration using the data handling system installed in the instrument itself that incorporates comparing the peak area of compound with the peak area of the known quantity of internal standard (5 μ g/g of methyl nonadecanoate for *n*-alkanes; 5 α -cholestane for *n*-alcohols+sterols). The carbon preference index (CPI) for *n*-alkanes was obtained by the ratio of the sum of odd carbon number homologues in the range of C₂₃₋₃₃ to the sum of even carbon number in the same range; and for *n*-alkanols, it is the ratio of the sum of even carbons in the range of C₂₂₋₃₂ to the sum of odd carbon numbers in the given range (Eglinton and Hamilton, 1967; Cranwell, 1973; Rieley et al., 1991). ACL for *n*-alkanes and *n*-alkanols was calculated using Poynter et al., 1989 equation. The recovery based on the standards for *n*-alkanes (C₂₀ to C₂₉) and *n*-alkanols (C₂₄ to C₃₀) + phytol + brassicasterol was >91 % and >87 % , respectively.

3. Results

The radiocarbon dating (Table 1) provided an age-model for the upper 1.2 m section of the core CC2-GCEq2 (Figure 3) that corresponds to the last 33 kyr with a sedimentation rate of \sim 3 cm/ky. The $\delta^{18}\text{O}_{G.ruber}$ vary from -0.8 to -2.4 ‰ with a glacial-interglacial gradient of 1.6 ‰ (Table 2 and Figure 4). After subtracting the global ice-volume effect of 1.2 ‰ (Shackleton, 2000), the remainder of 0.4 ‰ appears to have caused by changes in the equatorial surface water climatology. The MIS 1/2 boundary in the $\delta^{18}\text{O}_{G.ruber}$ time-series is identified at 13.2 ka BP. The MIS 2/3 boundary is marked at 29 ky BP following the LR-04 (Lisiecki and Raymo, 2005). The heaviest $\delta^{18}\text{O}_{G.ruber}$ (-0.8 \pm 0.1 ‰) representing the LGM occurs between 21.4 – 17.1 ky BP and the Holocene optimum condition ($\delta^{18}\text{O}_{G.ruber}$ of -2.27 ‰) was attained by 10.7 ky BP. The LGM is characterised by the heaviest $\delta^{18}\text{O}_{G.ruber}$ (-1 \pm 0.1 ‰) and covers a time-span of 9.7 ky (25.4 – 15.7 ka BP). The deglaciation period is evident by rapid depletion of $\delta^{18}\text{O}_{G.ruber}$ between 15.7 ka BP and 10.7 ka BP.

The C_{org} and N_{Tot} vary between 0.4 and 1.3 %, and 0.1 and 0.2 %, respectively (Table S1). The LGM average C_{org} is 1.04 % as against the 0.6 % of Holocene average (Table 2). Few lipids which could be considered as indicators of export production such as *n*-alkanes, *n*-alkanols, and sterols also exhibit distinctly higher average contents in the LGM section (av. 502, 258 and 17 ng/g, respectively) than in Holocene section (av. 378, 149, and 4 ng/g, respectively) (Table 2). The C/N ratios (Table S1) during the Holocene range from 5.1 to 7.2 (av. 6.4: Table 2), which are closer to the Redfield Ratio (RR) of marine phytoplankton (6.6), whereas, the C/N ratios in the LGM are relatively higher (7.4-8.2: av. 7.8). The $\delta^{13}C_{\text{org}}$ vary from -22.8 ‰ to -19 ‰ with relatively heavier $\delta^{13}C_{\text{org}}$ (Average -19.8 ‰) during the LGM as compared to the Holocene (-21.5 ‰) (Table 2). The lipids specific to marine production, such as phytol and brassicasterol are enriched in the LGM section (Phytol 4.6 to 7.8 and Brassicasterol 2.3 to 7.3 ng/g) as compared to the Holocene (1.3 to 2.3 and 0.8 to 3.3 ng/g, respectively) (Table S2). The average C_{23} - C_{33} *n*-alkanes and C_{22} - C_{32} *n*-alkanols are distinctly higher by more than factor of 2 in the LGM than in the Holocene section (174 and 75 ng/g and 88 and 22 ng/g, respectively) (Table 2, Figure 5a,b). Similarly, the CPI of *n*-alkanes and *n*-alkanols are higher in LGM sections (Table S3) with an average of 3.7 and 5.7 respectively (Table 2) than in the Holocene sections (Av. 2 and 4.9 respectively). Although the ACL of *n*-alkanes and *n*-alkanols exhibit marginal differences, they are relatively higher in the LGM sections (30 and 25.8) as against the Holocene values of 29.4 and 25.4, respectively (Table 2). There are few parameters showing some overlapping values during the deglacial period, which are expected during the climate transition. We do not consider further the variations found within the deglaciation period (~16 – 10 ky BP) as the biogeochemical response of the EIO during major and rapid adjustments in the climate system is not clearly known.

4. Discussion

The variable preservation of organic matter in the studied core causing C_{org} variation may be ruled out because the location of the sediment core falls within well oxygenated equatorial deep water regime (>3500 m) and there are no evidences for suboxic/anoxic conditions in this region during the past. Therefore, two times higher content of C_{org} in the LGM sediment than in the Holocene sediment (~1 % and 0.6 % respectively: Table 2, Figure 4) suggests significantly increased productivity during the LGM. The increased C_{org} in sediment could also be due to enhanced input of terrestrial carbon (soil organic matter) by either enhanced fluvial or eolian actions. In the present scenario, the strengthening of summer monsoon rain dependent Ganges-Brahmaputra and peninsular rivers discharging largest sediment load in to the open Indian Ocean via Bay of Bengal (BoB) is unlikely, because, there have been several studies demonstrating the weakening of summer

monsoons during the LGM, which were replaced by intensified winter monsoons (Anderson and Prell, 1993; Rostek et al., 1997; Prins and Weltje, 1999; Clemens and Prell, 2003; Banakar et al., 2005). The intensification of winter monsoons (north-easterly cold and dry winds) could have enhanced the supply of soil-carbon from the Indian subcontinent to the open ocean. The higher C/N ratios and $\delta^{13}\text{C}_{\text{org}}$ during the LGM (~ 8 and -19.8 ‰ respectively: Table 2, Figure 4) than during the Holocene (~ 7 and -21.3 ‰) suggest that the soil-carbon input to the ocean in fact was higher during the LGM. The increased $\delta^{13}\text{C}_{\text{org}}$ during the LGM (Table 2) also indicates that the terrestrial C_{org} input must have been dominated by the C4-plant ($\delta^{13}\text{C}_{\text{org}} \sim 12$ ‰) rather than the C3-plant ($\delta^{13}\text{C}_{\text{org}} \sim -27$ ‰), along with increased marine production having average $\delta^{13}\text{C}_{\text{org}} \sim -20$ ‰ (see Hoeffs, 1996). The estimation of terrestrial component based on binary mixing of two end-members, the marine organic matter (with C/N ~ 6.6) and the terrestrial organic matter (with C/N ~ 30) (Walsh et al., 1981) indicates <10 % of terrestrial component in the studied sediment. However, this mixing is complex as three different C_{org} components (Marine, C3- and C4-Terrestrial plants) are mixed with variable proportions. Additionally, the re-mineralization of organic matter in oxygenated deep-water of the EIO may have further reduced the fidelity of C_{org} and C/N ratios as indicators of palaeo-productivity. Therefore, more robust indicators are required for realistic assessment of marine versus terrestrial organic matter contributions to the sediment.

4.1. Terrestrial carbon input and monsoon intensity

The high molecular weight *n*-alkanes in the range of C_{23} to C_{33} showed predominance of odd *n*-alkanes at C_{23} , C_{27} , C_{29} , C_{31} and C_{33} (Figure 5A,B). In the high molecular weight *n*-alkanols (C_{23} to C_{32}) the predominance of even carbon numbers C_{22} , C_{24} , C_{26} , C_{28} , C_{30} and C_{32} was observed (Figure 6A,B). The observed high molecular *n*-alkanes and *n*-alkanols are characteristic of vascular terrestrial plants (Brassell et al., 1978; Clark and Blumer., 1967; Yunker et al., 2011; Simoneit, 1986, 1989; Cranwell and Volkman, 1981; Rieley et al., 1991; Rommerskirchen et al., 2006). It is therefore, possible to unscramble the proportion of terrestrial plant-biomass in the present sediment core by estimating C_{23-33} *n*-alkanes and C_{22-32} *n*-alkanols. The C_{23-33} *n*-alkanes and C_{22-32} *n*-alkanols are ~ 35 % of their total contents in the LGM section and ~ 20 % in the Holocene section (Table S3), which clearly indicate the presence of significant proportion of terrestrial organic matter in the equatorial sediment unlike that presented by mixing model of the C/N ratios. In addition, the CPI of *n*-alkanes and *n*-alkanols characterising the terrestrial plant-biomass (Cooper and Bray 1963; Rieley et al., 1991) also exhibit distinct increase during the LGM (Figure 8). The higher ACL that differentiates terrestrial-C3 plants from -C4 plants (Gagosian and Peltzer, 1986; Rommerskirchen et al., 2006), along with higher C/N ratios and $\delta^{13}\text{C}_{\text{org}}$ during the LGM (Figure 4) than during the

Holocene together suggest that the increased terrestrial organic matter input during the LGM was dominated by C4 type organic matter. This observation is consistent with both colder climate (CLIMAP, 1976; Hays et al., 1976) and intensified Indian winter monsoons during the LGM (Beaufort, 1996; Banakar et al., 2005; 2010; and references therein), where the former conditions favour the growth of C4-plants, and the latter conditions favour transport of terrestrial organic matter to the open ocean surrounding the Indian Subcontinent.

4.2. *Marine productivity variation and implications to westerly jet intensity*

To understand the productivity changes in the EIO, it is necessary to examine the time-series of lipid proxies characteristic of only the marine production. The phytol and brassicasterol are synthesised exclusively through marine photosynthesis (Volkman, 1986; Wakeham et al., 1997). These two lipids interestingly exhibit enrichment during the LGM by a factor of ~3 as compared to the Holocene (Table 2 and Figure 9) and confirms the previous reports of glacial high productivity in the northern Indian Ocean (Cayre and Bard, 1999; Schulte et al., 1999; Beaufort, 1996; Tamburini et al., 2003; Banakar et al., 2005). However, the proportion of brassicasterol in total sterols does not exhibit a clear increase during the LGM (Figure 10) in accordance with its absolute abundance (Figure 9). This discordance may suggest that the diatom production was not overwhelming during LGM compared to other sterol sources added to the sediment.

The significantly increased equatorial productivity in the Indian Ocean might have contributed to the drawdown of atmospheric CO₂ during the LGM providing a positive feedback for the glacial cooling. The probable mechanism that might have triggered significant increase in the equatorial production during the LGM could be attributed to the intensification of inter-monsoon WJs (Beaufort et al., 1997), because the intensification of WJ is expected to induce upwelling (shoaling of thermocline) along its periphery (see Figure 1) and advection of upwelled nutrients towards equator. Further, a recent modelling study (Liu et al., 2007) has shown intensification of equatorial westerly winds (WJs) during LGM causing shoaling of thermocline in central-western Indian Ocean forcing negative IOD events having ~15% enhanced amplitude and increased frequency than the Present. Thus the increased LGM productivity in EIO might have been caused by a combination of internally connected a) intense shoaling of thermocline in the central-western Indian Ocean due to intensified WJs along with enhanced negative IOD events and b) intensification of winter monsoons as evident in significantly increased input of terrestrial organic matter that could have added to the EIO's nutrient pool.

5. Conclusions

The organic geochemical multi-proxy study of a radiocarbon dated sediment core from the Equatorial Indian Ocean independently confirms the previous observations of increased productivity in the tropical Indian Ocean during the LGM. The index-lipids for terrestrial and marine organic matter suggest that the LGM productivity was significantly increased along with the supply of C4 dominated terrestrial organic matter to the open ocean culminating in enhanced sedimentary C_{org} . The increased glacial Equatorial Indian Ocean productivity appears to be the result of combination of significantly intensified Wyrki Jets enhancing the nutrient levels in the photic layer, and the increased input of soil-nutrients from Indian sub-continent by the intensified winter monsoons.

Acknowledgements

The sediment core used in this study was collected on board R.V.A.A. Sidorenko cruise under Cobalt-Crust Project funded by the Ministry of Earth Sciences, Government of India. The manuscript has been benefited by the critical comments and useful suggestions of two anonymous reviewers and David J.W. Piper, Co-Editor in Chief. N. B Bhosle helped in setting up lipid extraction experiments. VRP thanks UGC-CSIR for fellowship. The discussions with D. Shankar on westerly jet dynamics was helpful. Supriya Karapurkar assisted in oxygen isotope measurements. Supriya Karapurkar of NIO assisted with oxygen isotope measurements. Mitzi D'Martino of the University of Arizona and Von de Borg of the Utrecht University measured the samples for radiocarbon dates. This is NIO contribution No..

References

- Anderson, D. A., Prell, W. L., 1993. A 300 kyr record of upwelling off Oman during the late Quaternary: evidence of the Asian southwest monsoon. *Palaeoceanography* 13, 607-621.
- Banakar, V. K., Oba, T., Chodankar, A. R., Kuramoto, T., Yamamoto, M., Minagawa, M., 2005. Monsoon related changes in sea surface productivity and water column denitrification in the Eastern Arabian Sea during the last glacial cycle. *Marine Geology* 219, 99-108.
- Banakar, V. K., Mahesh, B. S., Burr, G., Chodankar, A. R., 2010. Climatology of the Eastern Arabian Sea during the last glacial cycle reconstructed from paired measurement of foraminiferal $\delta^{18}O$ and Mg/Ca. *Quaternary Research* 73, 535-540.
- Beaufort, L., 1996. Dynamics of the monsoons in the equatorial Indian ocean over the last 260,000 years. *Quaternary International* 31, 13-18.

- Beaufort, L., Lancelot, Y., Camberlin, P., Cayre, O., Vincent, E., Bassinot, F., Labeyrie, L., 1997. Insolation cycles as a major control of Equatorial Indian Ocean Primary Production. *Science* 278, 1451.
- Bligh, E. G., Dyer, W. J., 1959. A rapid method of total lipid extraction and purification. *Canadian Journal of Biochemistry and Physiology* 37, 911-917.
- Brassel, S. C., Eglinton, G., Maxwell, J. R., Philp, R. P., 1978. Natural background of alkanes in the aquatic environment. In: O Hutzinger, L H van Lelyveld, B C J Zoeteman (eds); *Aquatic Pollutants: Transformation and Biological Effects*, Pergamon Press, Oxford, England 69-86.
- Cayre, O., Bard, E., 1999. Plankton foraminiferal and alkenone records of the last deglaciation from the eastern Arabian Sea. *Quaternary Research* 52, 337-342.
- Cayre, O., Beaufort, L., Vincent, E., 1999. Paleoproductivity in the Equatorial Indian Ocean for the last 260,000 yr: A transfer function based on planktonic foraminifera. *Quaternary Science Reviews* 18, 839-857.
- Chang, C. P., Harr, P., Ju, J., 2001. Possible role of Atlantic circulation on weakening of Indian monsoon rainfall-ENSO relationship. *Journal of Climate* 14, 2376-2380.
- Clark, R. C. Jr., Blumer, M., 1967. Distribution of n-paraffins in marine organisms and sediment. *Limnology and Oceanography* 12, 79-87.
- Clemens, S. C., Prell, W. L., 2003. A 350,000 year summer monsoon multi-proxy stack from the Owen Ridge, Northern Arabian Sea. *Marine Geology* 201, 35-51.
- CLIMAP Project Members., 1976. The surface of the ice- age earth. *Science* 191,1131-1144.
- Cooper, J., Bray, E., 1963. A postulated role of fatty acids in petroleum formation. *Geochimica et Cosmochimica Acta* 27, 1113-1127.
- Cranwell, P. A., 1973. Chain length distribution of *n*-alkanes from lake sediments in relation to post glacial environment change. *Freshwater Biology* 3, 259-265.
- Cranwell, P. A., Volkman, J. K. 1981. Alkyl and steryl esters in recent lacustrine sediment; *Chemical Geology* 32, 29-43.
- Danzeglocke, U., Jois, O., Wenninger, B., 2008. CalPal 2007 online. <http://www.calpal-online.de/>, 2008-10-05.
- Eglinton, G., Hamilton, R. J., 1967. Leaf epicuticular waxes. *Science* 156, 1322-1335.
- Gadgil, S., Vinayachandran, P. N., Francis, P. A., 2003. Droughts of the Indian summer monsoon: Role of clouds over the Indian Ocean. *Current Science* 85, 1713-1719.
- Gagosian, R. B., Peltzer, E. T., Merrill, J. T., 1986. The importance of atmospheric input of terrestrial organic material to deep sea sediments. *Organic Geochemistry* 10, 661-669.
- Haake, B., Ittekkot, V., Rixon, T., Ramaswamy, V., Nair, R. R., Curry, W. B., 1993. Seasonality and inter-annual variability of particle fluxes to the deep Arabian Sea. *Deep Sea Research I* 40, 1323-1344.
- Harji, R. R., Yvenat, A., Bhosle, N. B., 2008. Sources of hydrocarbons in sediments of the Mandovi estuary and the Marmugoa harbour, west coast of India, *Environment International* 34, 959-965.

- Hayes, J. D., Imbrie, J., Shackleton, N. J., 1976. Variations in the earth's orbit: pacemaker of the ice ages. *Science* 194, 1121-1132.
- Hoefs, J., 1996. In: *Stable Isotope Geochemistry*, 4th edition Springer Heidelberg, pp 134.
- Hong, Y. T., Hong, B., Lin, Q. H., Zhu, Y. X., Shibata, Y., Hirota, M., Uchida, M., Leng, X. T., Jiang, H. B., Xu, H., Wang, H., Yi, L., 2003. Correlation between Indian Ocean summer monsoon and North Atlantic climate during the Holocene. *Earth and Planetary Science Letters* 211, 371-380.
- Krishna Kumar, K., Kleeman, R., Cane, M. A., Rajagopalan, B., 1999. Epochal changes in Indian monsoons-ENSO precursors. *Geophysical Research Letters* 26, 75-78.
- Kurian, S., Agnihotri, R., Borole, D. V., Naqvi, S. W. A., Farreira, A. M., Vale, C., 2009. Possible solar control on primary production along the west coast on decadal to centennial timescale. *Journal of Quaternary Science* 24, 109-116.
- Lisiecki, L. E., Raymo, M. E., 2005. A Pliocene-Pleistocene stack of 57 globally distributed benthic $\delta^{18}\text{O}$ records. *Paleoceanography* 20, PA1003: doi: 10.1029/2004PA001071.
- Liu, X., Liu, Z., Clemens, S., Prell, W., Kutzbach, J., 2007. A coupled model study of Glacial Asian Monsoon Variability and Indian Ocean Dipole. *Journal of Meteorological Society of Japan* 85, 1-10.
- Nagura, M., McPhaden M., 2010. Wyrki jet dynamics: Seasonal variability. *Journal of Geophysical Research* 115, C07009, doi:10.1029/2009JC005922.
- Poynter, J. G., Farrington, P., Brassel, S. C., Eglinton, G., 1989. Aeolian-derived higher plant lipids in the marine sedimentary records: links with paleoclimate. In: Leinen M, Sarnthein M (Eds); *Palaeoclimatology and Palaeometeorology; Modern and Past Patterns of Global Atmosphere Transport*, Kluwer, pp. 435-462.
- Prins, M. A., Weltje, G. J., 1999. End member modelling of siliciclastic grain size distribution: The late Quaternary record of eolian and fluvial sediment supply to the Arabian Sea and its paleoclimatic significance; In: *Numerical experiments and stratigraphy: Recent advances in Stratigraphic and Sedimentologic computer simulations*, SEPM Special publications No. 63 pp: 91-111.
- Rieley, G., Collier, R. J., Jones, D. M., Eglinton, G., 1991. The biogeochemistry of Ellesmere Lake, UK-I: source correlation of leaf wax inputs to the sedimentary lipid record, *Organic Geochemistry* 17, 901-912.
- Rommerskirchen, F., Eglinton, G., Dupont, L., Rullkotter, J., 2006. Glacial/interglacial changes in southern Africa: compound-specific $\delta^{13}\text{C}$ land plant biomarker and pollen records from southeast Atlantic continental margin sediments. *Geochemistry, Geophysics, Geosystems* 7, Q08010. doi:10.1029/2005GC001223.
- Rostek, F., Bard, E., Beaufort, L., Sonzogni, C., Ganssen, G., 1997. Sea surface temperature and productivity records for the past 240 kyr in the Arabian Sea. *Deep-Sea Research, Part II* 44: 1461-1480.
- Roy, S. S., 2011. The role of the North Atlantic Oscillation in shaping regional scale peak seasonal precipitation across Indian subcontinent. *Earth interactions* doi: 10.1175/2010 EI 339.1 V. 15, 1-13.

- Schubert, C.J., Villanueva, J., Calvert, S.E., Cowie, G.L., von Rad, U., Schulz, H., Berner, U., Erlenkeuser, H., 1998. Stable phytoplankton community structure in the Arabian Sea over the past 200,000 years. *Nature* 394, 563–566.
- Schulte, S., Bard, E., 2003. Past changes in biologically mediated dissolution of calcite above the chemical lysocline recorded in Indian Ocean sediments. *Quaternary Science Reviews* 22, 1757–1770.
- Schulte, S., Rostek, F., Bard, E., Rullkotter, J., Marchal, O., 1999. Variations of oxygen-minimum and primary productivity recorded in the sediments of the Arabian Sea. *Earth and Planetary Science Letters* 173, 205-221.
- Schulz, H., von Rad, U., Erlenkeuser, H., 1998. Correlation between Arabian Sea and Greenland climate oscillations of past 110000 years. *Nature* 393, 54-57.
- Senan, R., Sengupta, D., Goswami, B. N., 2003. Intraseasonal “monsoon jets” in the equatorial Indian Ocean. *Geophysical Research Letters* 30, 1750, doi:10.1029/2003GL017583.
- Shackleton, N. J., 2000. The 100,000 year ice-age cycle identified and found to lag temperature, carbon dioxide and orbital eccentricity. *Science* 289, 1897-1902.
- Simoneit, B. R. T., 1986 Characterization of organic constituents in aerosols in relation to their origin and transport: a review; *International Journal of Environmental Analytical Chemistry* 23: 207-237
- Simoneit, B. R. T., 1989 Organic matter of the troposphere. V. Application of molecular marker analysis to biogenic emissions into the troposphere for source reconciliations; *Journal of Atmospheric Chemistry* 8: 251-275
- Tamburini, F., Föllmi, K. B., Adatte, T., Bernasconi, S. M., Steinmann, F., 2003. Sedimentary phosphorus records from the Oman Margin: new evidence of high productivity during glacial periods. *Paleoceanography* 18, 15-1–15-14.
- Volkman, J. K., 1986. A review of sterol markers for marine and terrigenous organic matter. *Organic Geochemistry* 9, 83-99.
- Volkman, J. K., 2006. Lipid markers for marine organic matter In: Volkman, J K (Ed.), *Handbook of Environmental Chemistry, Volume 2: Reactions and Processes 2 (N)*. Springer, Berlin, pp. 27-70.
- Wakeham, S. G., Lee, C., Hedges, J. I., Hernes, P. J., Peterson, M. L., 1997a. Molecular indicators of diagenetic status in marine organic matter. *Geochimica et Cosmochimica Acta* 61, 5363–5369.
- Walsh, J. J., Premuzic, E. T., Whitley, T. E., 1981. Fate of nutrient enrichment on continental shelves as indicated by C/N content of bottom sediments In: *Echohydrodynamics* J C J Nihoul (Ed). Elsevier, pp: 13-49.
- Wyrski, K., 1973. An equatorial jet in the Indian Ocean. *Science* 181, 262-264.
- Yunker, M. B., Macdonald, R. W., Snowdon, L. R., Fowler, B. R. 2011. Alkane and PAH biomarkers as tracers of terrigenous organic carbon in Arctic Ocean sediments, *Organic Geochemistry*, doi: 10.1016/j.orggeochem.2011.06.007.

Captions to Figures:

Figure 1. Location of CC2-GCEq2 sediment core used in the present study (filled circle) shown on the November 1996 wind map of the Northern Indian Ocean (Source: www.coaps.fsu.edu), to represent the period of occurrence of Wyrтки Jets. A highly simplified dynamics of the Wyrтки Jet is schematically shown on right hand side. The eastward propagating Wyrтки Jets have their highest energy along the equator and decay outwards. This should result in convergence (thermocline deepening) and high sea level along its propagation (Equator), while divergence (thermocline shoaling) and lowering of sea level along its periphery.

Figure 2. The seasonal climatology of the Northern Indian Ocean where Wyrтки Jet activity is distinctly seen along the Equator during May (Spring) and November (Fall) seasons of the year (upper panel: Nagura and McPhaden, 2010). The bottom panel shows corresponding months' chlorophyll-a distribution (Source: SeaWiFS image, <http://las.nio.org>), which is highest during the activity of Wyrтки Jets (May and November) at CC2/GCEq2 sediment core location (white circle).

Figure 3. Radiocarbon age versus Depth plot for the upper 121 cm of the CC2-GCEq2 sediment core. The maximum age at 121 cm is 33.7 ky BP. Broken lines mark the 100 cm depth and its corresponding age (32.8 ky BP) considered in the present study.

Figure 4. Composite of time-series of $\delta^{18}\text{O}_{G.ruber}$ (A), C_{org} (B), C/N (C) and $\delta^{13}\text{C}_{org}$ (D) in CC2GCEq2 sediment core. The filled arrow heads on vertical axis of the panel-A denote the radiocarbon dated sections along with their corresponding calendar age in ky BP. The broken horizontal lines running across all the panels denote the marine oxygen isotope boundaries between Holocene and LGM, which remain same for figures 7 through 10. (OM – Organic Matter).

Figure 5. GC-MS profile of *n*-alkanes obtained for subsection 12-14 cm (7.8 ky BP-representing Holocene) (A), and subsection 42-46 cm (18.4 ky BP-representing Last Glacial Maximum) (B) in CC2/GCEq2. (ISTD: Internal Standard).

Figure 6. GC-MS profile of *n*-alkanols and sterols obtained for subsection 12-14 cm (7.8 ky BP-representing Holocene) (A), and subsection 42-46 cm (18.4 ky BP-representing Last Glacial Maximum) (B) in CC2/GCEq2. (ISTD: Internal Standard). Phytol peak at retention time 20.0-20.5 minutes and Brassicasterol peak at retention time 33.0 minutes are shown as 1 and 2 respectively.

Figure 7. Temporal variation of, A) *n*-alkanes (Total = C_{16-33} and high molecular weight = C_{23-33}), and B) *n*-alkenols (Total = C_{14-32} and high molecular weight = C_{22-32}).

Figure 8. The past variation of Carbon Preference Index (CPI) and Average Chain Length (ACL) of *n*-alkanes (A) and *n*-alkanols (B).

Figure 9. Time-series of phytol and brassicasterol, which are the index lipids for marine production.

Figure 10. Temporal variation of percent proportion of brassicasterol in total sterols

Table 1. Details of AMS radiocarbon dating of CC2/GCEq2 Sediment Core*

Laboratory Sample Ref. ID	Section Depth (cm)	Measured Age (yr BP)	Error (±y)	Calendar Age (cal yr BP)	Error ±y
X10253	2	5159	43	5204	105
X10254A	11	6644	46	6892	64
X10255A	21	10659	58	11605	180
X10256	31	12309	99	13591	156
X10257	43	15628	84	18262	240
X10258	62	19070	140	22079	334
X10259	91	28500	380	32467	395
X10260	121	29960	350	33717	388

*Measured at NSF-Arizona University AMS Facility on 6 October 2008; Reservoir Age = 600 y

Table 2. Climate period averaged elemental, isotopic and molecular abundance in sediment core CC2/GCEq2

Period Ky BP	C _{org} %	C/N	$\delta^{13}\text{C}_{\text{Org}}$ ‰ PDB	n- alkanes	n- alkanols	Sterols	C23-33	C22-32	CPI n- alkanes	CPI n- alkanols	ACL n- alkanes	ACL n- alkanols	Phytol	Brassicasterol
				ng/g dry wt. sediment									ng/g dry wt. sediment	
Holocene	0.6	6.2	-21.3	378	149	4	88	22	2.0	29.4	4.9	25.4	1.9	1.9
LGM	1.0	7.8	-19.8	502	258	17	174	75	3.7	30.0	5.7	25.8	5.8	4.9

Figure 1

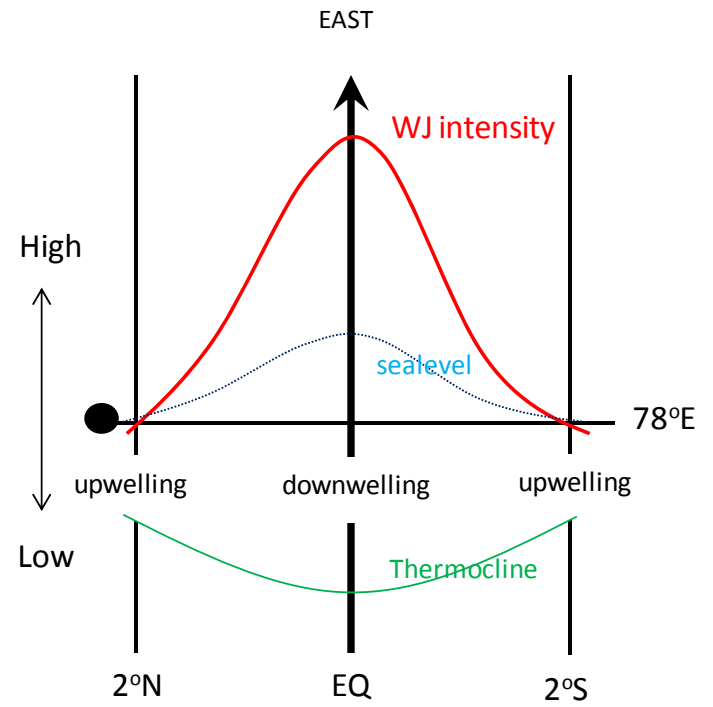
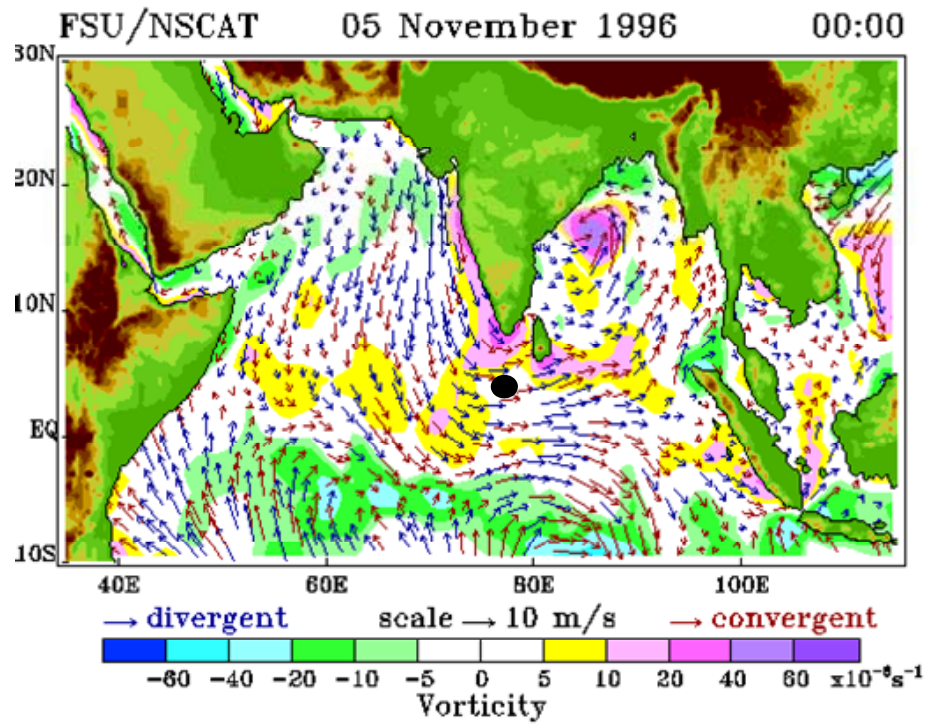


Figure 2

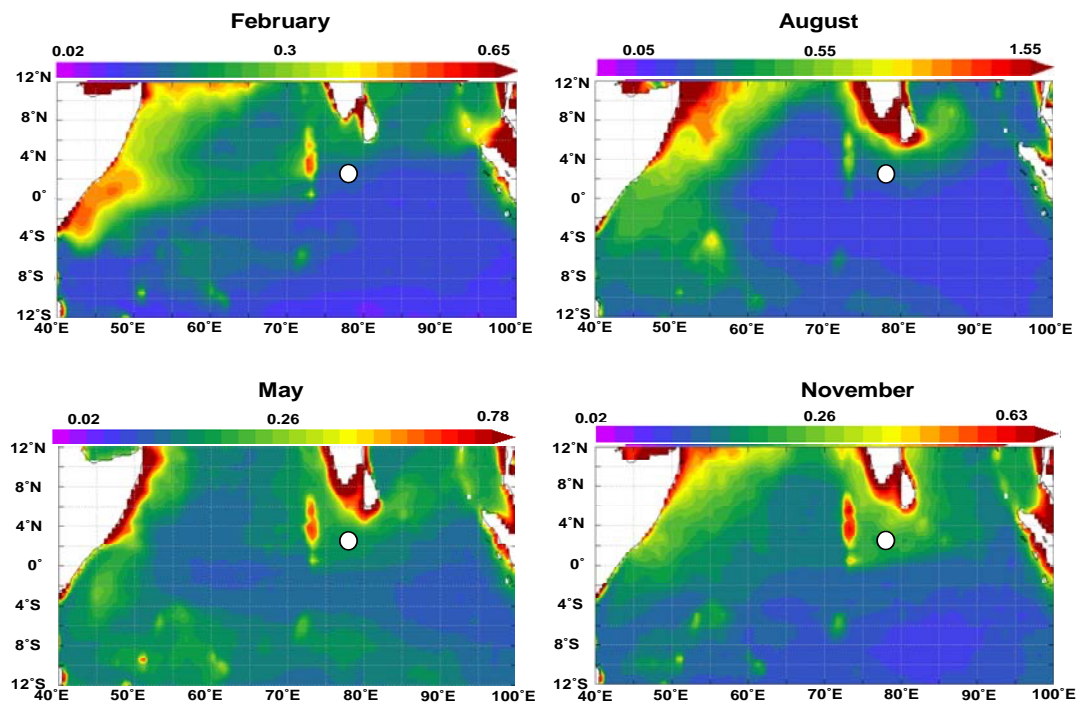
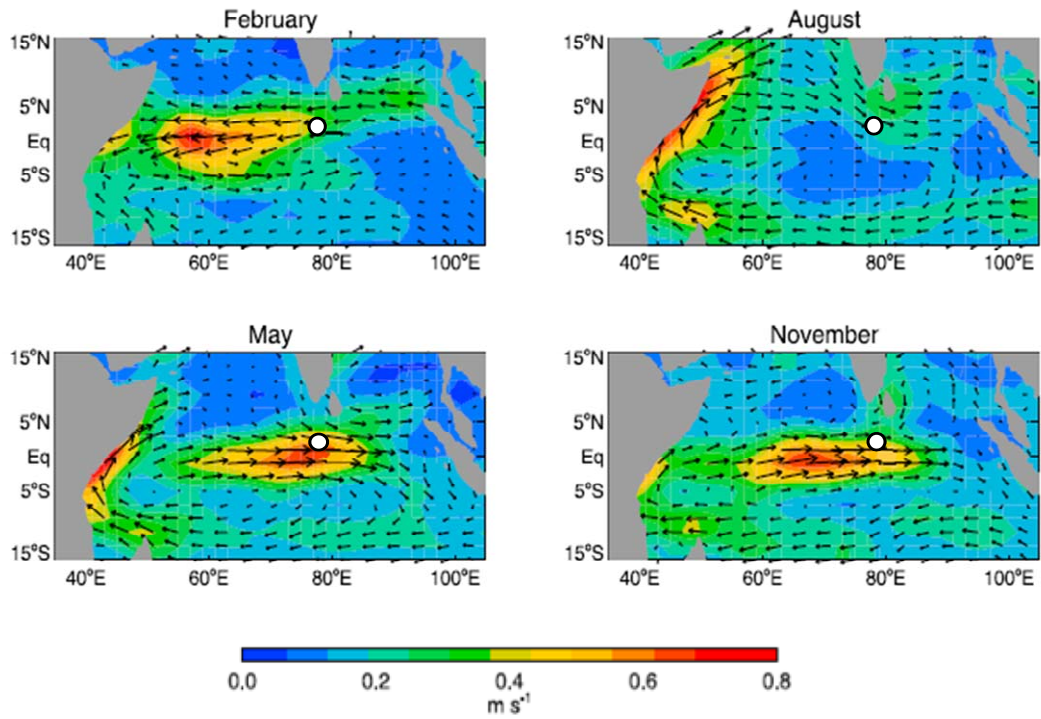


Figure 3

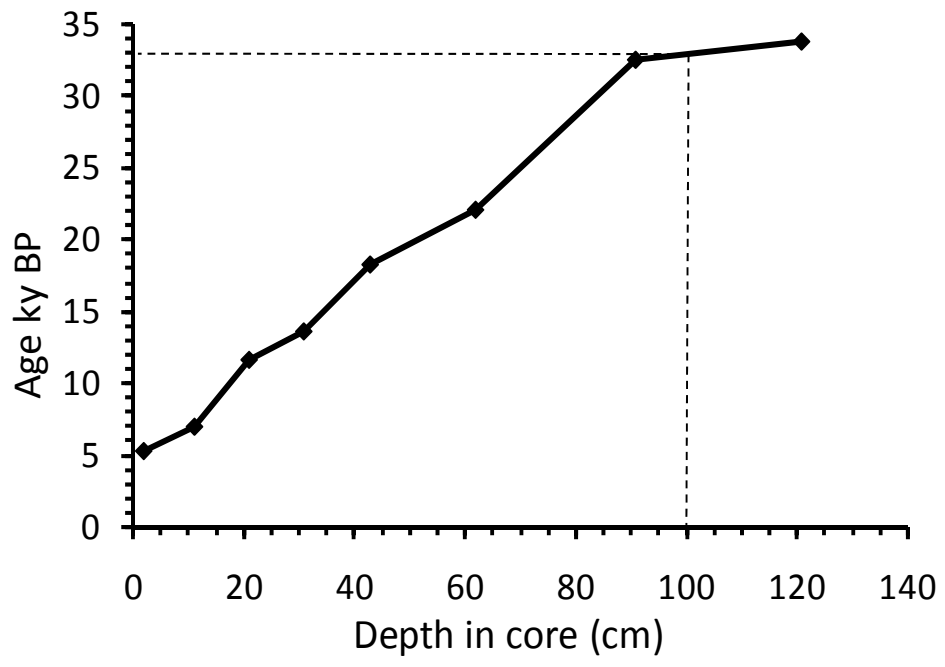


Figure 4

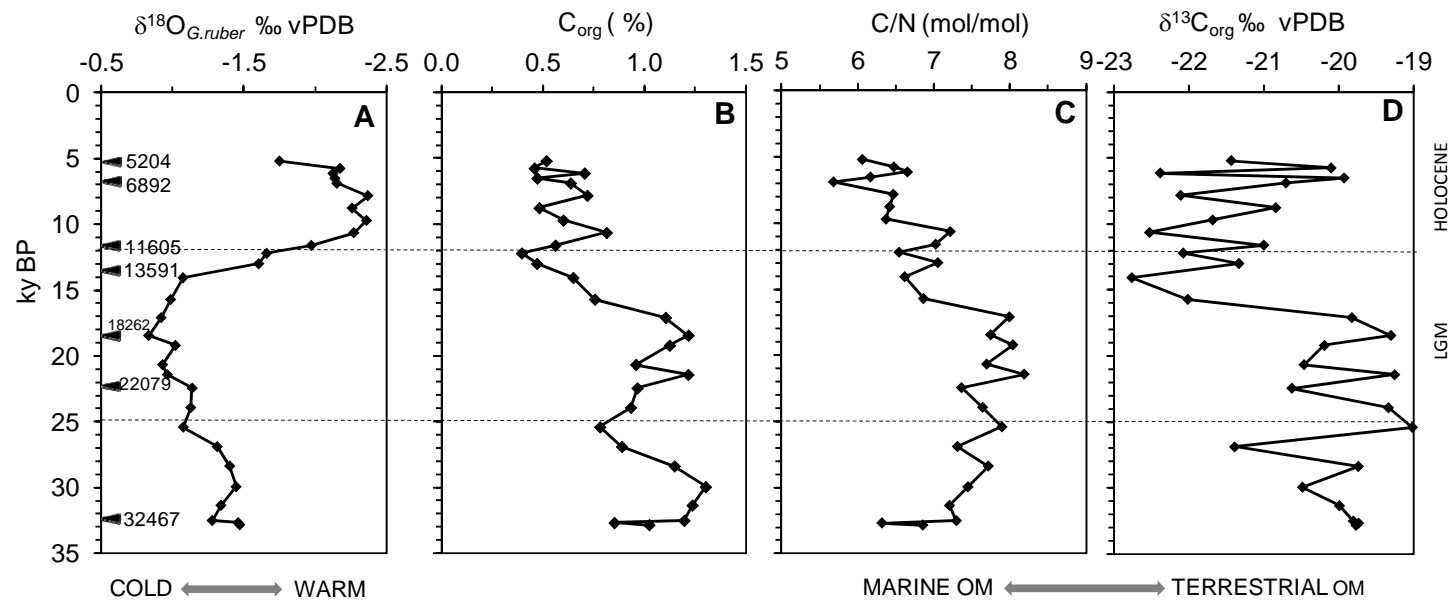


Figure 5

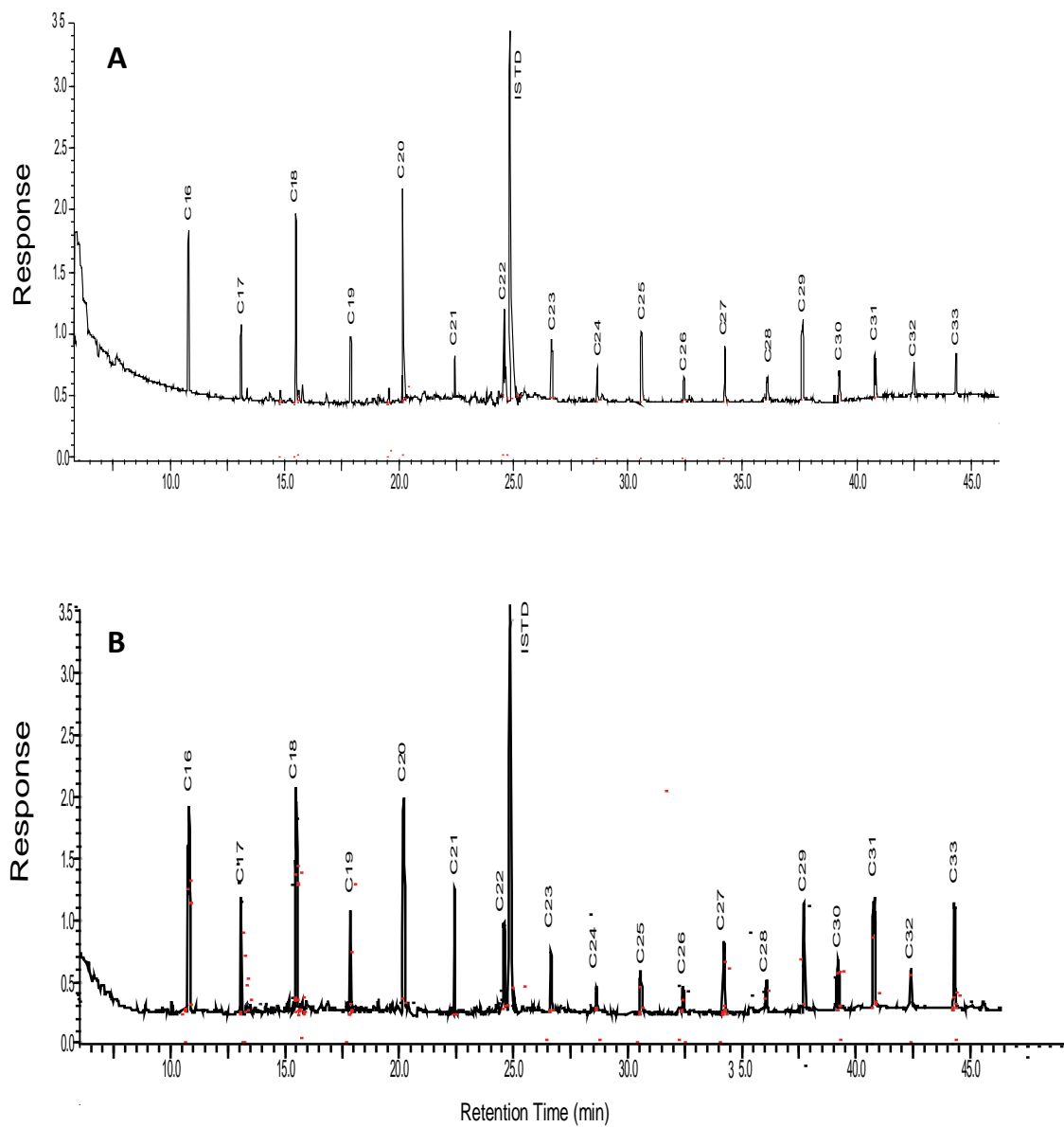


Figure 6

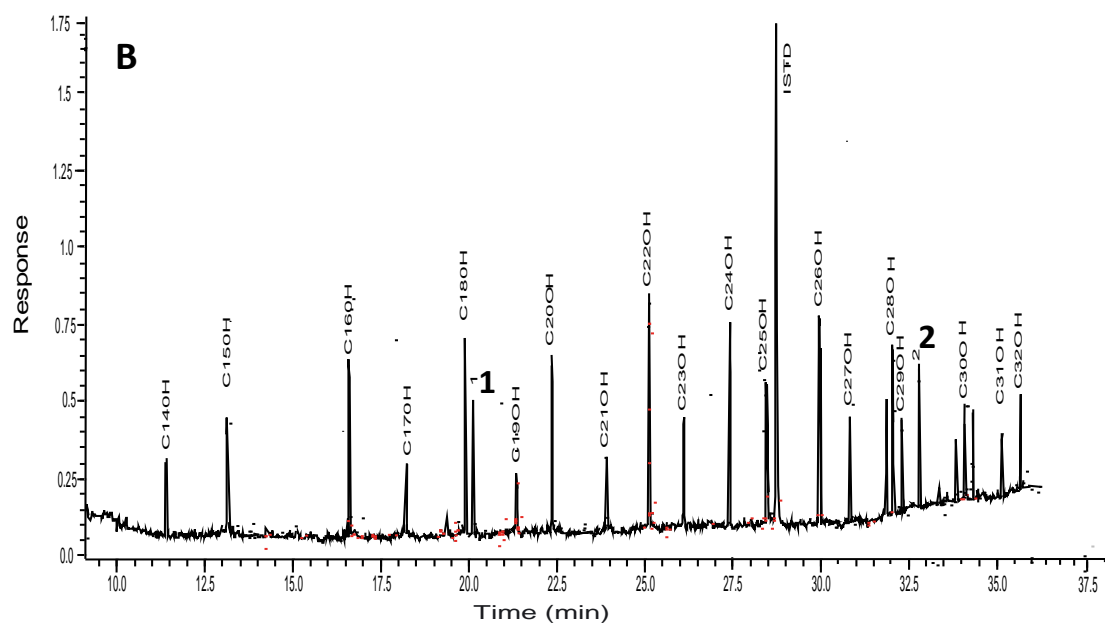
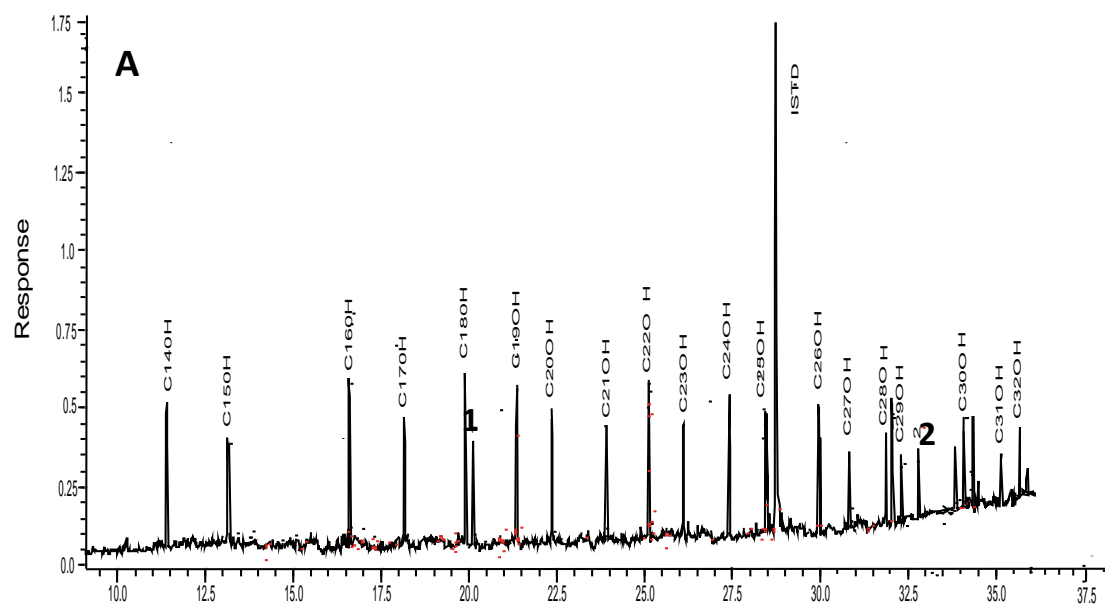


Figure 7

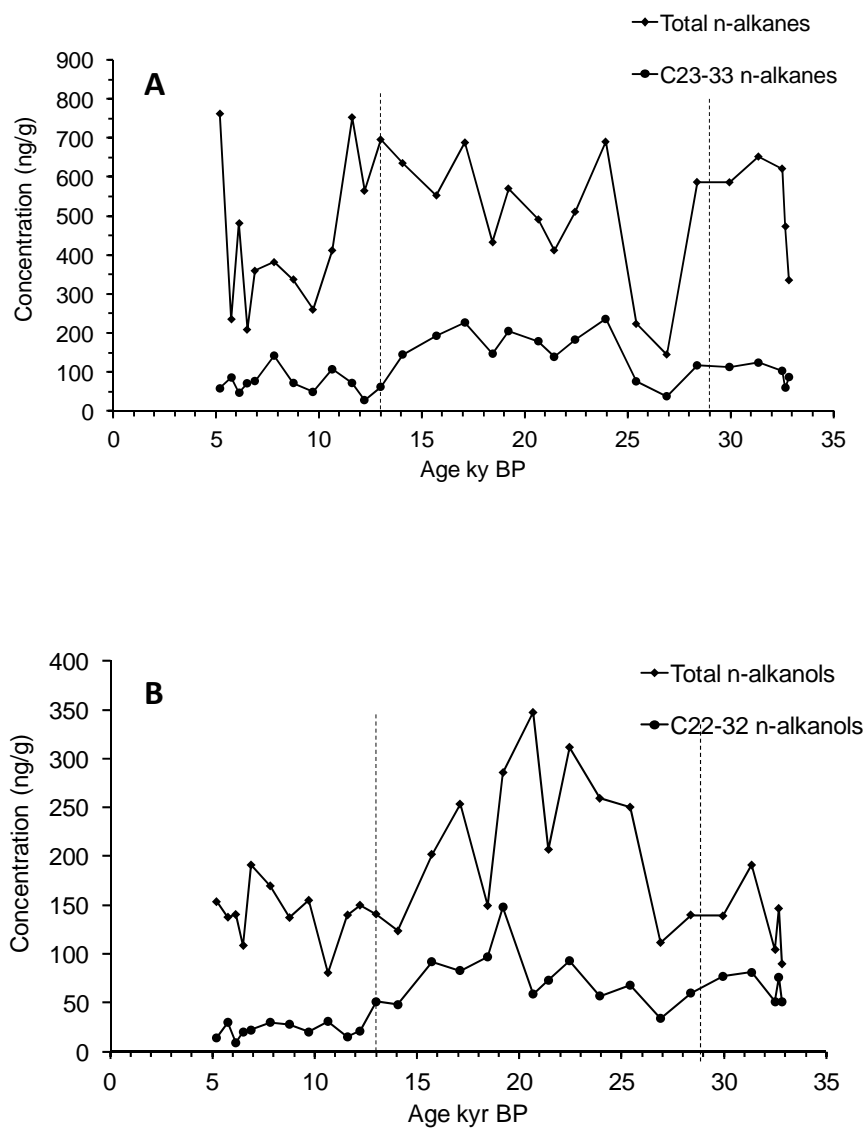


Figure 8

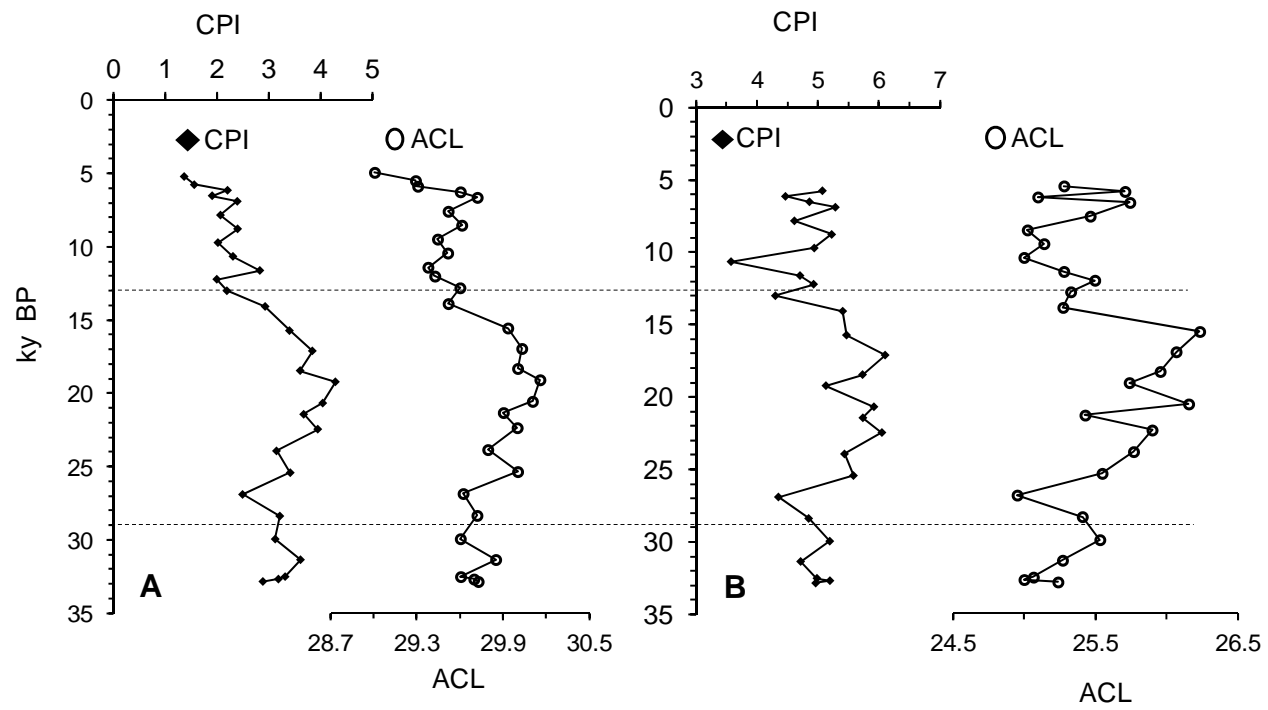


Figure 9

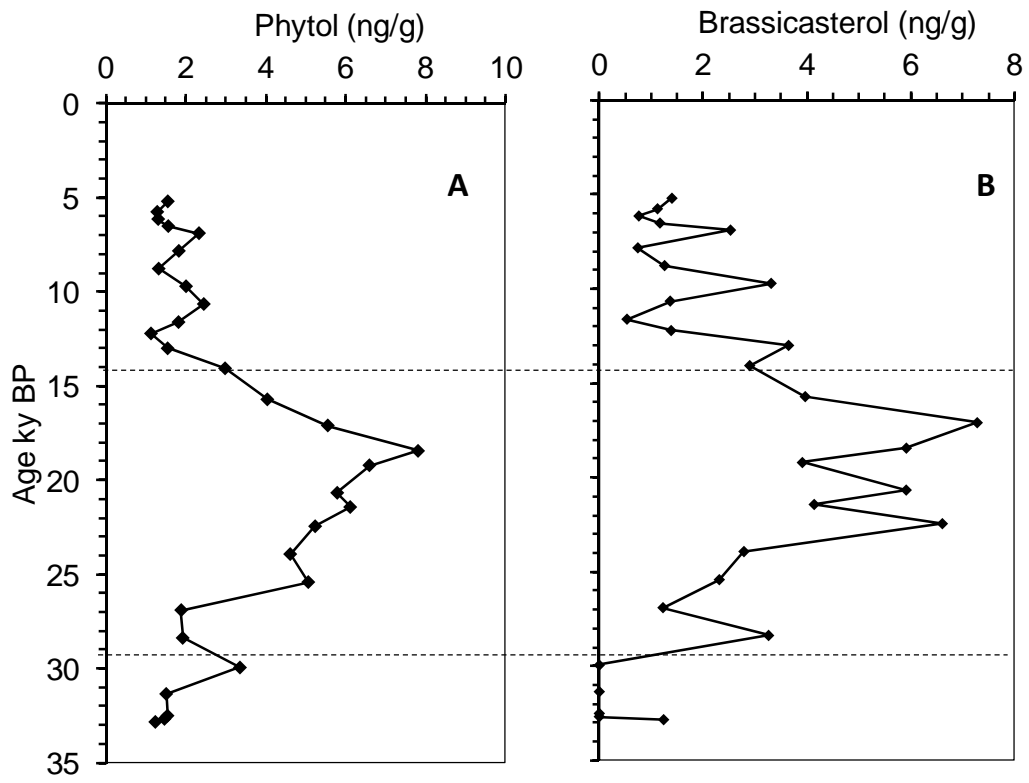
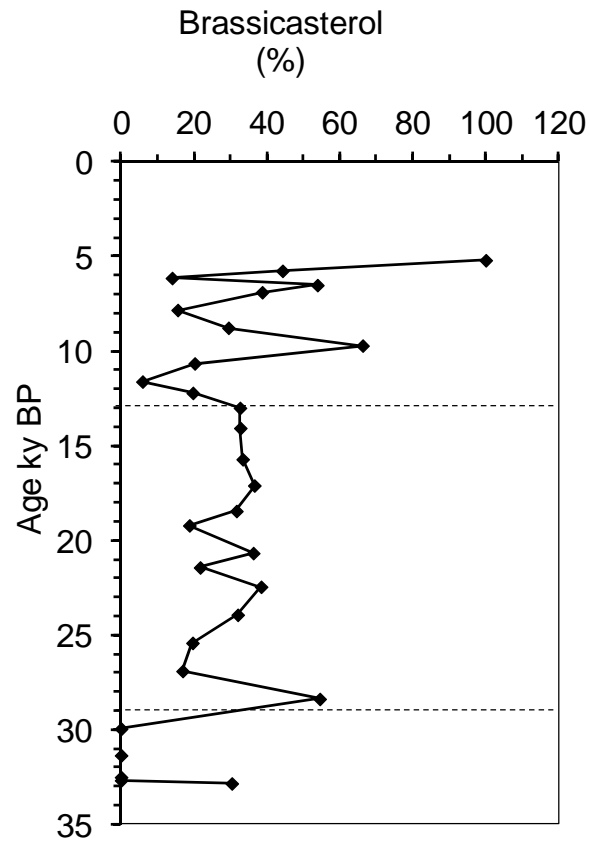


Figure 10



**Table S1. Time-series of isotopic and C_{org} and N_{tot} in CC2GCEq2 sediment core.
(Bold fonts indicate the radiocarbon dated sections and their corresponding calendar age)**

Depth (cm)	Calendar Age (yr BP)	$\delta^{18}\text{O}_{G. ruber}$ ‰ vPDB	C _{org} (%)	N _{Tot} (%)	C/N (mol/mol)	$\delta^{13}\text{C}_{org}$ ‰ vPDB
2	5.2	-1.75	0.5	0.1	6.1	-21.4
5	5.8	-2.18	0.5	0.1	6.5	-20.1
7	6.1	-2.13	0.7	0.1	6.7	-22.4
9	6.5	-2.14	0.5	0.1	5.2	-19.9
11	6.9	-2.15	0.6	0.1	5.7	-20.7
13	7.8	-2.37	0.7	0.1	6.5	-22.1
15	8.8	-2.26	0.5	0.1	5.1	-20.8
17	9.7	-2.34	0.6	0.1	6.4	-21.7
19	10.7	-2.27	0.8	0.1	7.2	-22.5
21	11.6	-1.97	0.6	0.1	7.0	-21.0
24	12.2	-1.66	0.4	0.1	6.5	-22.1
28	13.0	-1.60	0.5	0.1	7.1	-21.3
31	13.6	NA	NA	NA	NA	NA
32	14.1	-1.07	0.6	0.1	6.6	-22.8
36	15.7	-0.99	0.8	0.1	6.9	-22.0
40	17.1	-0.92	1.1	0.2	8.0	-19.8
43	18.3	NA	NA	NA	NA	NA
44	18.5	-0.83	1.2	0.2	7.7	-19.3
48	19.2	-1.02	1.1	0.2	8.0	-20.2
54	20.7	-0.93	1.0	0.1	7.7	-20.5
60	21.4	-0.96	1.2	0.2	8.2	-19.3
63	22.1	NA	NA	NA	NA	NA
64	22.5	-1.14	1.0	0.2	7.4	-20.6
68	23.9	-1.13	0.9	0.1	7.6	-19.3
72	25.4	-1.08	0.8	0.1	7.9	-19.0
76	26.9	-1.31	0.9	0.1	7.3	-21.4
80	28.4	-1.40	1.1	0.2	7.7	-19.7
84	30.0	-1.45	1.3	0.2	7.4	-20.5
88	31.4	-1.34	1.2	0.2	7.2	-20.0
91	32.5	-1.28	1.2	0.2	7.3	-19.8
96	32.7	-1.46	0.9	0.2	6.3	-19.7
100	32.8	-1.47	1.0	0.2	6.9	-19.8
121	33.7	NA	NA	NA	NA	NA

NA = Not analyzed; All values rounded to nearest decimal

Table S2. Distribution of various lipid fractions* in CC2/GCEq2

Age ky BP	Total n-alkanes	Total n-alkanols	Total sterols	Phytol	Brassi- casterol
5.2	762	153	1.4	1.6	1.4
5.8	235	138	2.5	1.3	1.1
6.1	481	140	5.5	1.3	0.8
6.5	209	109	2.2	1.6	1.2
6.9	360	191	6.5	2.3	2.5
7.8	381	170	4.8	1.8	0.7
8.8	337	137	4.3	1.3	1.3
9.7	260	155	5.0	2.0	3.3
10.7	412	81	6.8	2.5	1.4
11.6	753	140	9.1	1.8	0.5
12.2	565	150	7.0	1.1	1.4
13.0	696	141	11.2	1.5	3.6
14.1	635	124	8.9	3.0	2.9
15.7	553	202	11.9	4.0	4.0
17.1	688	253	19.9	5.6	7.3
18.5	433	149	18.7	7.8	5.9
19.2	570	286	20.9	6.6	3.9
20.7	491	347	16.3	5.8	5.9
21.4	412	207	19.1	6.1	4.1
22.5	511	312	17.2	5.2	6.6
23.9	690	259	8.7	4.6	2.8
25.4	224	250	11.8	5.1	2.3
26.9	145	112	7.3	1.9	1.2
28.4	587	140	6.0	1.9	3.3
30.0	586	139	5.2	3.4	0.0
31.4	652	191	2.8	1.5	0.0
32.5	621	104	1.4	1.5	0.0
32.7	473	147	0.9	1.5	0.0
32.8	336	90	4.1	1.2	1.2

* = Concentration in ng/g of dry sediment

Total *n*-alkanes=C₁₆₋₃₃; Total *n*-alkanols=C₁₄₋₃₂

Table S3. Time-series of lipids characteristic of terrestrial organic matter present in CC2GCEq2

Age ky BP	<i>n</i> -alkanes				<i>n</i> -alkanols			
	C ₂₃₋₃₃ ng/g	C ₂₃₋₃₃ %	CPI C ₂₃₋₃₃	ACL	C ₂₂₋₃₂ ng/g	C ₂₂₋₃₂ %	CPI C ₂₂₋₃₂	ACL
5.2	58	8	1.4	29.0	14	9	4.3	25.4
5.8	86	37	1.6	29.3	30	21	5.1	25.3
6.1	47	10	2.2	29.3	9	7	4.5	25.7
6.5	71	34	1.9	29.6	20	18	4.9	25.1
6.9	77	21	2.4	29.7	22	12	5.3	25.7
7.8	142	37	2.1	29.5	30	18	4.6	25.5
8.8	72	21	2.4	29.6	28	21	5.2	25.0
9.7	49	19	2.0	29.4	20	13	4.9	25.1
10.7	107	26	2.3	29.5	31	38	3.6	25.0
11.6	72	10	2.8	29.4	15	11	4.7	25.3
12.2	28	5	2.0	29.4	21	14	4.9	25.5
13	62	9	2.2	29.6	51	36	4.3	25.3
14.1	145	23	2.9	29.5	48	39	5.4	25.3
15.7	193	35	3.4	29.9	92	46	5.5	26.2
17.1	227	33	3.8	30.0	83	33	6.1	26.1
18.5	147	34	3.6	30.0	97	65	5.7	26.0
19.2	205	36	4.3	30.2	148	52	5.1	25.7
20.7	179	36	4.0	30.1	59	17	5.9	26.2
21.4	139	34	3.7	29.9	73	35	5.7	25.4
22.5	183	36	3.9	30.0	93	30	6	25.9
23.9	236	34	3.1	29.8	57	22	5.4	25.8
25.4	76	34	3.4	30.0	68	27	5.6	25.5
26.9	38	26	2.5	29.6	34	30	4.4	25.0
28.4	117	20	3.2	29.7	60	43	4.8	25.4
30	113	19	3.1	29.6	77	55	5.2	25.5
31.4	124	19	3.6	29.8	81	43	4.7	25.3
32.5	103	17	3.3	29.6	51	49	5	25.1
32.7	60	13	3.2	29.7	76	52	5.2	25.0
32.8	87	26	2.9	29.7	51	57	5	25.2

ACL = Average Chain Length; CPI = Carbon Preference Index; concentration on dry sediment basis